Mutual Coupling Analysis for a SKA1-LOW Station

Paola Di Ninni[1], Mirko Bercigli[2], Pietro Bolli[1], Giuseppe Virone[3], Stefan J. Wijnholds[4]
[1]Osservatorio Astrofisico di Arcetri - Istituto Nazionale di Astrofisica, OAA-INAF, Florence, Italy
[2]Ingegneria Dei Sistemi S.p.A., IDS, Pisa, Italy
[3]Istituto di Elettronica e di Ingegneria dell'Informazione e delle Telecomunicazioni - Consiglio Nazionale delle Ricerche, IEIIT-CNR, Turin, Italy
[4] Netherlands Institute for Radio Astronomy, ASTRON, Dwingeloo, The Netherlands

***Abstract*—The modelling of the antenna patterns represents one of the main challenges for the instrumental calibration of radio telescopes composed by antennas randomly distributed. In this work, the electromagnetic characterization of a single station of the low-frequency instrument of the Square Kilometre Array (SKA) radio telescope operating from 50 to 350 MHz is reported. The station is assumed to be composed by Log Periodic antennas. The effects of mutual coupling on the complex embedded element patterns and on the array beam are investigated by means of a full-wave electromagnetic analysis. The accuracy of a simplified, mutual coupling-free approach is presented as well.**

***Index Terms*—Low frequency aperture array, antenna mutual coupling, full-wave electromagnetic model, Square Kilometre Array.**

I. INTRODUCTION

The Square Kilometre Array (SKA, https://www.skatelescope.org/) is a new generation radio telescope planned to address some of the fundamental questions in astrophysics. SKA will be the most sensitive radio telescope ever conceived to study the Universe in the centimeter and meter wavelengths. To date, the first phase of SKA is well-defined and will be made up of two different instruments: SKA1-MID (from 350 MHz to 14 GHz) and SKA1-LOW (from 50 MHz to 350 MHz).

SKA1-LOW is a low-frequency aperture array (LFAA) system characterized both by a large number of small antennas spread over large distances and digital beamforming. SKA1-LOW will consist of 512 stations, each composed of 256 antennas.

Several Aperture Array Verification Systems (AAVS) have been constructed by the Aperture Array Design and Construction (AADC) consortium to validate the readiness of the technology planned for SKA1-LOW [1]. Initial results indicate that the station calibration may become a challenging and resource consuming task due to the large differences between the embedded element patterns. In fact, whilst a random antennas distribution assures smoothness of the array pattern without grating lobes, this design causes a significant diversity in the patterns of each individual antenna due to the mutual coupling effects. The lack of unicity of the mutual coupling forces to carry out an accurate EM characterization of the antenna patterns, hopefully validated by experimental system like, for instance, drone measurements [2]. At the same time, for some specific array configurations, a simplified modelling procedure neglecting mutual coupling effects can turn out to be accurate enough, thereby relaxing the expensive computational time required by the full-wave approach.

The focus of this contribution is, in the first place, to investigate mutual coupling effects for a station composed of 256 Log Periodic antennas elements randomly distributed. To this end, the complex embedded element patterns and the array patterns have been simulated between 50 and 350 MHz in far-field (FF) regime by means of a full-wave EM analysis. These results are compared to the patterns achievable using a simplified model based on an isolated antenna.

The contribution is organized as follows: the layout of a SKA1-LOW station is described in Section II, the EM simulator is introduced in Section III. Finally, the numerical results are reported in Section IV, while the conclusions are drawn in Section V.

II. SKA1-LOW STATION

A. Station geometry

The SKA1-LOW station will be composed of 256 elements randomly distributed in a circle with 38-m diameter. The antenna element planned for SKA1-LOW is a Log Periodic Dipole Antenna measuring two orthogonal linear polarizations, called SKALA4 [3]. This design comes from an intensive optimization process of previous SKALA designs carried out by the AADC consortium [4]. The antennas will be oriented with polarizations aligned along East-West and North-South directions. The antenna positions used in this contribution reflect the layout already used in the AAVS1 system (see Fig. 1). This antenna layout is not the final layout of the SKA1-LOW station.

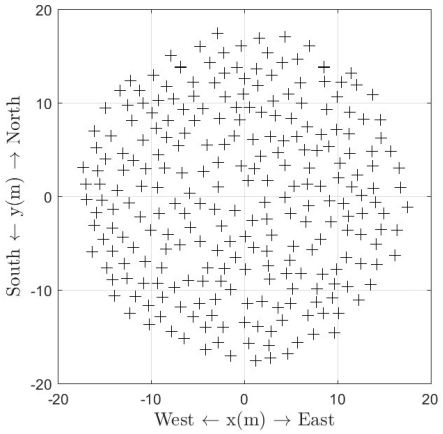

Fig. 1. Distribution of the 256 elements within the simulated station.

The sparseness degree of the array is given as the average of the minimum distances between two antennas (d) over the operating wavelength (λ). The limit between a sparse and a dense array corresponds to the ratio d/λ being equal to 0.5. For the AAVS1 distribution, d turns out to be 1.6 m (± 0.2 m standard deviation) which sets a frequency of about 95 MHz as the frequency where the AAVS1 array changes from a dense (lower frequencies) to a sparse array (higher frequencies).

B. SKALA4-AL Antenna

Each arm of the dual-polarized SKALA4 antenna is formed by 16 dipoles for a total height from the ground mesh of about 2.1 m [3]. The top 15 dipoles have an upward triangular shape, while the bottom one is a bow-tie dipole. The SKALA4 antenna is characterized by a close boom solution.

One of the possible implementations of the SKALA4 conceptual design is the so-called SKALA4-AL antenna, whose main features are: 50-Ω input impedance, aluminium alloy material and antenna grounding. Such characteristics assure several advantages like, for instance, easy testability with standard radio-frequency instruments, low weight, good corrosion resistance and good properties in terms of electrical discharge. Two prototypes of this antenna have been fabricated by the Italian company Sirio Antenne and have gone through several experimental verifications including tests in a semi-anechoic chamber (see Fig. 2) and in the Western Australia where SKA1-LOW will be deployed.

III. FULL-WAVE SIMULATION

A. Galileo-EMT

The results presented in this contribution are obtained by full-wave simulations performed using the commercial software Galileo-ElectroMagnetic Toolkit (Galileo-EMT, https://www.idscorporation.com/pf/galileo-suite/). Galileo-EMT is a framework integrating a comprehensive set of interoperable solvers, pre-processing, post-processing and working procedures. The available solutions enable the user to select the most effective and efficient tool in each phase of the electromagnetic design process and for specific problems:

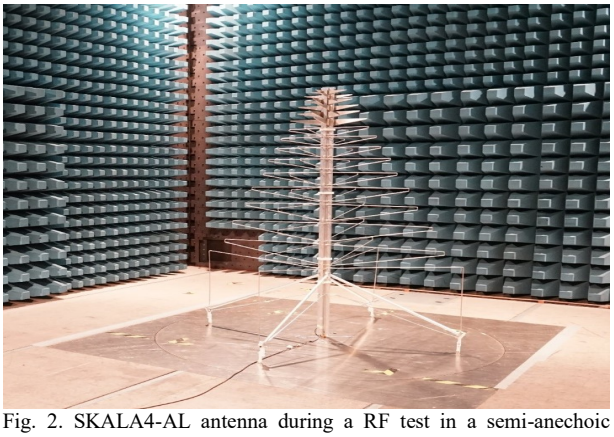
Fig. 2. SKALA4-AL antenna during a RF test in a semi-anechoic chamber.

- fast tools for preliminary design and fast prototyping
- a high fidelity simulation approach for detailed design and final verification
- optimized working procedures tailored to specific applications and problems.

All the available solvers have been validated by extensive physical testing campaigns (both using IDS physical testing solutions and measured data from research projects).

For this activity, the full-wave solver based on the Method of Moments (MoM) available in Galileo-EMT was used. This solver is accelerated by various methods including the Multi-Level Fast Multi-pole Algorithm (MLFMA) used for the simulation of the SKA1-LOW station.

In [5] other simulation techniques have been used to analyze similar large arrays.

B. Simulated data

The array EM model, simulated using the MoM-MLFMA based full-wave solver, is composed by 256 SKALA4-AL antennas placed over an infinite ideal, i.e. perfect electrically conducting (PEC), ground plane.

In order to minimize the uncertainty factors, the same EM model of the antenna was used for all frequencies. The model was meshed with a step suitable for the highest frequency (350 MHz). This results in an oversampled mesh for the lowest end of the frequency band (50 MHz). It is well known that this fact can lead to an ill-conditioned system with consequent convergence problems for the iterative methods used in the fast algorithms (e.g. MLFMA). The MoM-MLFMA code integrated in Galileo-EMT is provided, however, with a physics-based preconditioner (Multi-Resolution, MR) that eliminates this problem.

Each antenna of the array was modeled using 2942 Rao-Wilton-Glisson functions defined on triangle, 552 piecewise linear functions defined on wires and 84 junctions between triangles and wires. The number of unknowns for the entire

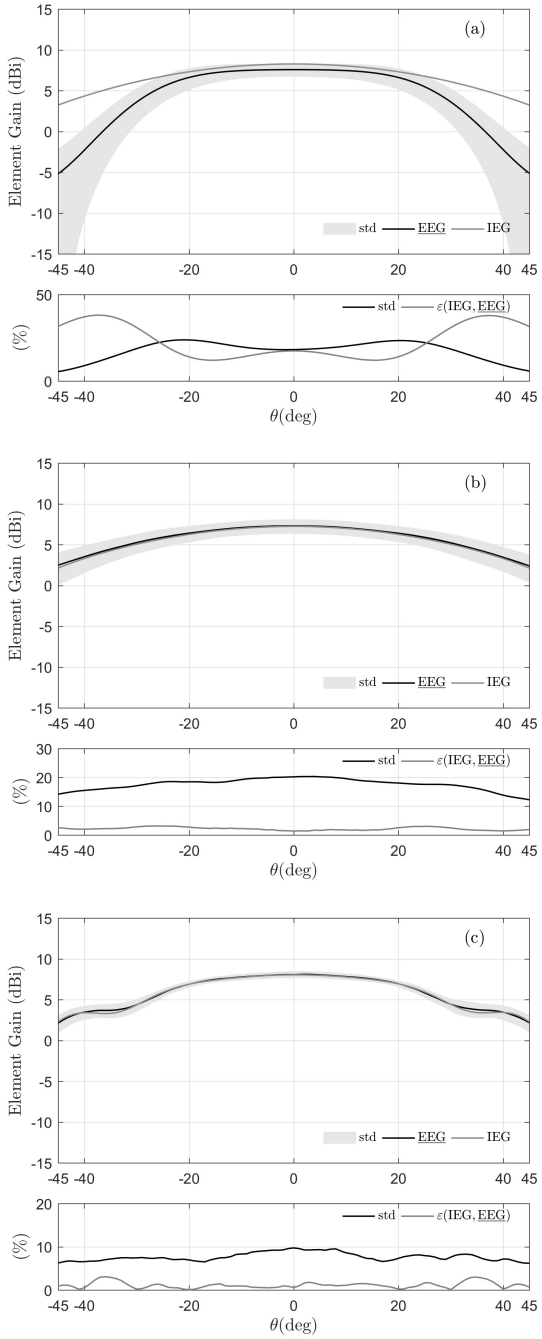

Fig. 3. Distribution of the 256 element gains along the E-plane at different frequencies: (a) 50, (b) 110 and (c) 350 MHz. The upper panels show the EEG distribution (grey shading), their average (black curve) and the IEG (grey curve). The bottom panels show the (percent) differences between EEG and IEG and the (percent) normalized standard deviation.

array was therefore 915,968 and the total number of ports was equal to 512 (two ports for each antenna).

By means of the MoM-MLFMA-MR solver, the 512 embedded patterns were calculated by feeding the active port through a V_g=1V and Z_g=50 Ω generator and closing all other array ports on a 50 Ω load. In addition to the patterns, the S-parameters (512x512 matrix) were also calculated using a 50 Ω reference impedance. Depending on the frequency, the computational cost of the simulation has varied from a minimum of 35 hours to a maximum of 74 hours with a peak RAM consumption equal to 151 GByte.

IV. Electromagnetic analysis results

In this Section, the EM analysis results from the full-wave approach are presented along the E-plane for the North-South oriented elements. The responses of the embedded elements have been compared to the response of the isolated element based on the mutual coupling-free approach. Both the phase of the co-polar electric field and the gain have been considered in this study. In the computation, we have assumed that the impedance of the receivers coupled with the array elements is 50 Ω at all frequencies. This assumption is justified since the impedance of the Low Noise Amplifier designed for the SKALA4-AL element varies slowly around the 50 Ω within the frequency band. Furthermore, the normalized array patterns have been evaluated in full-wave and mutual coupling-free approaches. In the first approach, the array pattern has been computed as the total electric field emitted by all antennas, while, in the simplified approach, the array factor-based method has been implemented. This method combines the isolated antenna pattern and the array factor of the station layout. In both cases, a uniform excitation for all antennas has been applied. Finally, the maps of the full-wave and simplified array patterns on the u-v plane are shown at 50 MHz.

A. Embedded element response

The effects of mutual coupling on the FF embedded element patterns are presented for the gain and the phase pattern. Fig. 3 shows the embedded element gain (EEG) at 50, 110 and 350 MHz. The cut is the E-plane, while the polar angle ranges between -45° and 45° representing the field of view of the radio telescope. The results of Fig. 3 are organized in two panels: the upper panel shows a black curve for the averaged EEGs (indicated as EEG), a grey curve for the isolated element gain (IEG) and a grey shading for the EEG distribution (given by the EEG curve plus and minus the standard deviation curve). The bottom panel shows the difference between IEG and EEG (indicated as ε) and the standard deviation of the EEG distribution (indicated as std). Both curves are normalized to the maximum of the EEG.

The standard deviation of the embedded element gains turns out to be more significant at 50 MHz than at 110 and 350 MHz. As shown in the bottom panels of Fig 3, the maximum values of the standard deviation in the field of view are 25%, 20% and 10% at 50, 110 and 350 MHz, respectively. The larger effect of mutual coupling at low frequency can be attributed to the close electrical spacing between the antennas. The standard deviation tends to vanish almost completely at 350 MHz, where the grey shading is quite indiscernible from the EEG and IEG curves.

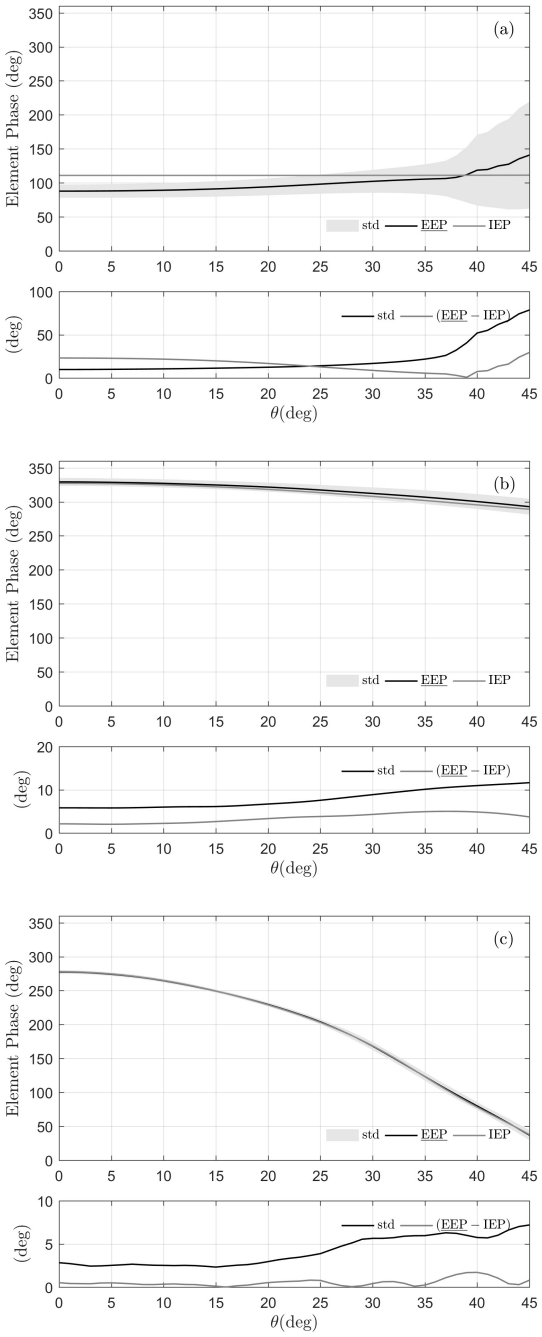

Fig. 4. Distribution of the 256 phases of the electric field along the E-plane at different frequencies: (a) 50, (b) 110 and (c) 350 MHz. The upper panels show the EEP distribution (grey shading), their average (black curve) and the IEP (grey curve). The bottom panels show both the differences between EEP and IEP and the standard deviation.

Besides, at 50 MHz the percent difference between EEG and IEG reaches the substantial value of 40% (corresponding to an error of 2 dB), while, again with the increasing frequency, EEG and IEG curves tend to superimpose on each other and the differences decrease to 4% (0.2 dB) and 3% (0.15 dB) at 110 and 350 MHz, respectively. This suggests that mutual coupling is almost completely negligible at the high end of the frequency band and a simpler, mutual coupling-free approach could produce quite accurate results.

In Fig. 4, the phases of the co-polar electric field emitted by each element are reported. The phases are referred to the base of each antenna. The results of Fig. 4 are organized similarly to the embedded element gains of Fig. 3. The upper panel shows a black curve for the average of the embedded element phases (indicated as EEP), a grey curve for the isolated element phase (IEP) and a grey shading for the EEP distribution. The bottom panel shows the difference between IEP and EEP and the standard deviation of the EEP distribution. The geometrical delays being removed, the distributions of the phases at the three frequencies account only for the mutual coupling effects. As for the embedded element gains, also for the phases the mutual coupling effect is definitively stronger at lower frequencies.

B. Array patterns

The normalized array patterns evaluated in the E-plane at 50, 110 and 350 MHz by means of both the non-approximated full-wave approach and the simplified mutual coupling-free approach are shown in Fig. 5. Besides, the percent differences between the two linearly normalized array patterns have been evaluated to quantify the agreement between the two procedures for the array pattern modelling.

In both cases, the array patterns have been computed as squared modulus of the co-polar electric field emitted by the array when an equi-amplitude and equi-phase feeding scheme is employed (corresponding to a main beam pointing towards the zenith direction).

For each frequency, the analysis results are organized in two panels. The upper panel shows the normalized array pattern from both the full-wave approach (black curve, FW) and the simplified approach (grey curve, AF). An additional panel shows the percent linear difference between the two sets of data.

The randomized distribution of the station elements ensures, as expected, the absence of grating lobes. As already seen for the embedded element responses, the comparison between two array patterns confirms that the mutual coupling effects decrease with increasing frequency. The maximum values of the differences are 1.6%, 0.6% and 0.5% at 50, 110 and 350 MHz, respectively. Such values correspond to an error of less than 0.1 dB, even at 50 MHz, showing that the randomization mitigates the large differences between the embedded element patterns.

Finally, in order to have a complete overview of the array pattern within 0° – 360° azimuthal angle, maps of the normalized array pattern have been made at 50 MHz. Fig. 6 shows the maps obtained by applying the full-wave and the simplified approach. The third map is computed as the linear differences between the previous maps and shows that the difference levels are highest in the the main beam area as confirmed by the difference in the bottom panel of the Fig. 5(a).

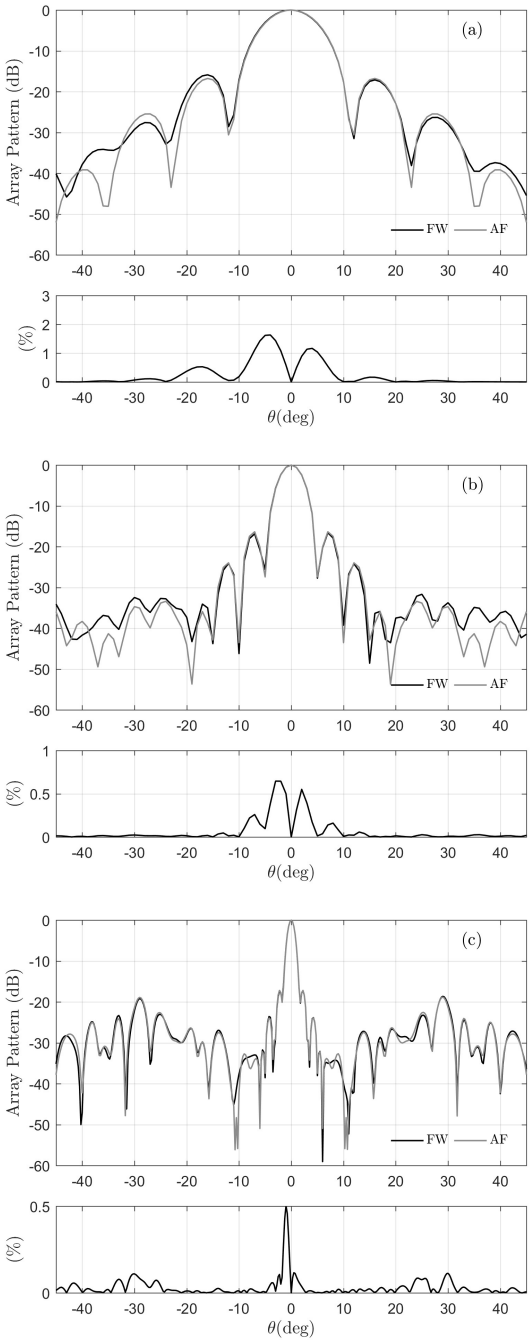

Fig. 5. Array patterns along the E-plane at different frequencies: (a) 50, (b) 110 and (c) 350 MHz. The upper panels show the full-wave array pattern (FW) and the array pattern based on the Array Factor procedure (AF). The bottom panels show the (percent) differences between the two array patterns.

V. CONCLUSION

A full-wave analysis of the embedded SKALA4-AL patterns distributed as envisaged for the SKA1-LOW radio telescope has been conducted. The analysis shows large inter-element variations in the element patterns at the lowest end of the frequency band while these significantly decrease toward 350 MHz. We have also verified that the array pattern can be computed with reasonable accuracy by using a simple array factor method.

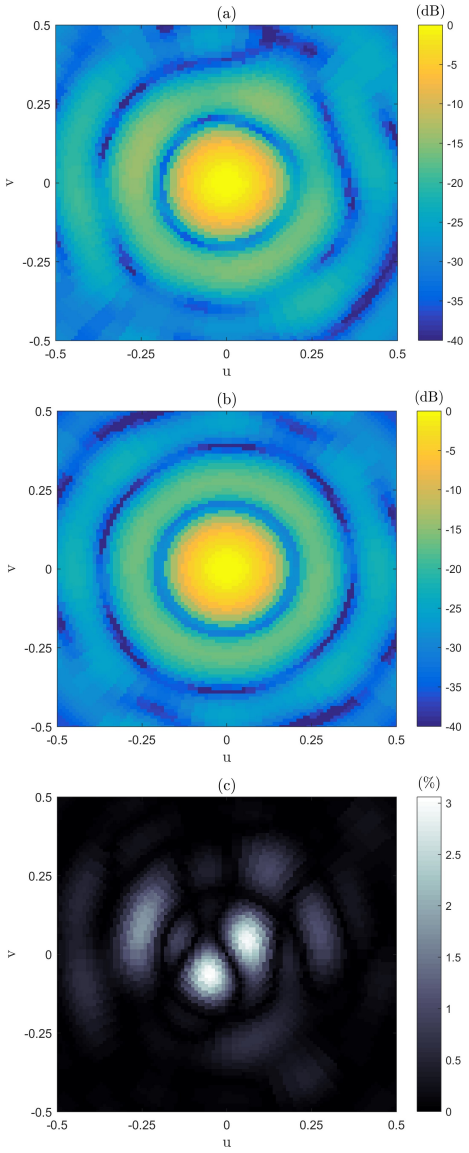

Fig. 6. Normalized array pattern at 50 MHz from full-wave (a) and mutual coupling-free approach (b). Percent differences shown in (c).

REFERENCES

[1] P. Benthem, et al. "The low frequency receivers for SKA 1-low: Design and verification," *32nd URSI GASS*, August 19-26, 2017.

[2] P. Bolli, et al. "In-Situ Characterization of International Low-Frequency Aperture Arrays by Means of an UAV-based System," *32nd URSI GASS*, August 19-26, 2017.

[3] E. de Lera-Acedo, et al., "SKA-1-LOW antenna selection - Description of the LPD antenna candidates", LFAA Antenna&LNA Work Package, AADC Consortium, 17 August 2017.

[4] E. de Lera-Acedo, et al., "SKALA, a log-periodic array antenna for the SKA-low instrument: design, simulations, tests and system considerations," *Experimental Astronomy*, vol. 39, 3, 2015.

[5] H. Bui-Van et al., "Fast and Accurate Simulation Technique for Large Irregular Arrays," *IEEE Trans. Antennas Propag.*, vol. 66, 4, 2018